Modeling In-Se amorphous alloys

Krisztian Kohary[1,*], Victor Burlakov[1], Duc Nguyen-Manh[2], and David Pettifor[1]
[1]Department of Materials, University of Oxford, Parks Road, Oxford, OX1 3PH, United Kingdom
[2]UKAEA Culham Division, Culham Science Centre, OX14 3DB, United Kingdom

ABSTRACT

The structure of amorphous In-Se alloys has been studied by a first principles tight-binding molecular dynamics technique using the program package PLATO (Package for Linear combination of Atomic Type Orbitals). The three-dimensional amorphous structures with different densities at different compositions were prepared by rapid quenching from the liquid phase. The characteristics of short-range order such as coordination numbers, radial and bond angle distribution functions, and electronic structure have been analyzed. Similar local bonding environments were found to be present in the amorphous phase as those in In-Se crystalline alloys, such as In_2Se_3, InSe, and In_4Se_3. The majority of bonds are heteropolar, but homopolar In-In and Se-Se bonds are also present in the amorphous phase. Indium is mainly four-fold coordinated, whereas on average selenium has either two or three nearest-neighbors. There is a large fluctuation in coordination numbers showing that amorphous In-Se alloys cannot be considered as network forming materials. In future, the material properties presented in this paper can serve as input parameters for continuum models that link crystallization processes to the underlying structure.

Keywords: InSe, phase-change materials, amorphous semiconductors, molecular dynamics

1. Introduction

Indium monoselenide (InSe) is a phase-change material: both the crystalline and amorphous phases are stable at room temperature [1]. Therefore, InSe has recently attracted considerable attention because of its potential application as a data storage medium [2-6]. The first phase-change experiments with materials based on In-Se alloys were performed by Nishida *et al*. [1]. In-Se alloys are also considered in other alternative technological applications such as solar cells and ionic batteries [7-11].

ln phase-change materials the digital information “0” or “1” is usually stored by amorphizing or crystallizing a small area (approximately with a diameter of the order of 100 nm) of the storage medium with the help of a laser pulse. Then the digital information is read by measuring the reflectivity of this small area. This is done again by a laser pulse, but this time with a smaller laser power in order to retain the amorphous or crystalline state of the measured area. Recently, however, it has been suggested that in phase-change materials electron beams could be used in order to store the digital information in a surface area with much smaller size than that generated by a laser pulse. The readout process would then also be via electrons, the proposed device being a thin film p-n junction [2-6].

Traditional phase-change storage mediums are based on alloy materials such as Ge-Sb-Te, In-Sb-Te, and Ag-In-Sb-Te [12]. These materials are widely used in current technological applications like CDs or DVDs. However, for devices using electron beams rather than a laser pulse, InSe has been suggested as a more suitable data storage medium [2-6].

As the amorphous phase of In-Se alloys has the potential for data storage at the nanoscale, it is necessary to understand its structural and electronic characteristics before the device applications can be optimized. In recent years, different compounds of crystalline and amorphous In-Se alloys have been studied extensively. The most important crystalline alloys are In_2Se_3, InSe, and In_4Se_3 [13], but other phases such as In_5Se_6 and In_6Se_7 have also been studied experimentally [14]. The structure of these materials is based on the local tetrahedral bonding configuration. It is therefore expected that this local tetrahedral bonding configuration is preserved in the amorphous phase. However, little is known about the details of the atomic structure of amorphous In-Se alloys. Amorphous In_2Se_3 and InSe structures were studied by Burian *et al.* using wide-angle X-ray scattering (WAXS) and extended X-ray absorption fine structure (EXAFS) techniques [15-17]. The goal of these experiments was to study the short-range order in amorphous films with the help of the radial distribution function. However, the radial distribution function provides only one-dimensional integrated information about the disordered structure. Therefore a detailed atomistic analysis is needed in order to better

*Email correspondence: krisztian.kohary AT materials.ox.ac.uk
http://www-mml.materials.ox.ac.uk/people/kohary.shtml

understand the physical properties of amorphous In-Se alloys. In this paper we report an *ab initio* study of the structural properties of amorphous compounds of In_2Se_3, InSe, and In_4Se_3.

2. Simulation details

A standard method to generate amorphous semiconductor structures is to perform rapid quench molecular dynamics simulations [18]. In such simulations the atomic structure is equilibrated slightly below or above the melting temperature. The temperature of the system is then gradually decreased to room temperature over a couple of picoseconds. Starting atomic configurations are typically randomly generated from the crystal structure. Generally three-dimensional cells with periodic boundary conditions are used in order to decrease surface effects. Systems normally contain up to 100-1000 atoms mainly depending on whether the interatomic forces are calculated by using classical two- and three-body potentials or by using very accurate *ab initio* program codes. The final structures need to be tested in order to check whether they represent an acceptable model of the amorphous structure.

We have performed first principles tight-binding molecular dynamics simulations to study amorphous In_2Se_3, InSe, and In_4Se_3 alloys. The three-dimensional amorphous structures in a cubic cell with periodic boundary conditions were generated by rapid quenching from the liquid phase. First, we equilibrated at 4000 K each simulation cell containing a randomly distributed initial atomic configuration for 1 ps simulation time with a 2 fs time step in order to generate random models which are independent of their initial states. Then the temperature was decreased from 4000 K to room temperature over 4 ps initially using a 2 fs time step until 2000 K after which a 1 fs time step was used.

The amorphous structures contained 65, 64, and 63 atoms for amorphous In_2Se_3, InSe, and In_4Se_3, respectively. For each composition the simulations were performed in the canonical (N,V,T) ensemble with densities of 5.0, 5.4, 5.8, and 6.2 g/cm^3, as the corresponding crystalline densities vary in this range: densities have been reported for In_2Se_3 around 5.4, 5.8, and 6.0 g/cm^3 and for InSe around 5.5 g/cm^3 [19]. Crystalline In_4Se_3 has a density close to 6.0 g/cm^3. In addition, amorphous In_2Se_3 films with 5.0 g/cm^3 were analyzed by Burian *et al.* [17].

We calculated the interatomic forces using the *ab initio* program code PLATO (Package for Linear combination of Atomic Type Orbitals) [20, 21]. In our calculations we used a double numeric basis set with polarization with $sps^*p^*d^*$ orbitals with a cutoff distance at 0.423 nm. We used a Γ-point sampling for the amorphous phase in our density functional theory (DFT) calculations within the local density approximation (LDA). We employed the exchange and correlation functional of Goedecker *et al.* [22] and the relativistic pseudopotentials of Hartwigsen *et al.* [23].

3. Amorphous In-Se structures

3.1. Radial distribution function

The radial distribution function $g(r)$ provides one-dimensional integrated information of the three-dimensional atomic arrangement. It reflects the nature of the short-range order in amorphous materials by having peaks at small atomic distances. Further peaks at larger atomic distances diminish reflecting the disordered structure of the material. It is customary to work with the reduced radial distribution function $G(r)$, which is defined by

$$G(r) = \frac{1}{r} 4\pi r^2 \left(\rho(r) - \rho_0\right) = \frac{g(r)}{r} - 4\pi r \rho_0 , \qquad (1)$$

where $\rho(r)$ is the density of atom centers at a distance r from an atom averaged over the network and ρ_0 is the average density. A comparison of the reduced radial distribution function of amorphous In_2Se_3 with a density of 5.0 g/cm^3 between our computer simulations and experiments of Burian *et al.* [17] is shown in Fig. 1. The predicted positions of the first and second peaks and the width of these peaks are in reasonable agreement with the experimental data. The radial distribution function of amorphous InSe with a density of 5.4 g/cm^3 is also shown in Fig. 1.

The reduced radial distribution function for different amorphous In-Se alloys with different densities show similar shape to the functions depicted in Fig. 1, as discussed in more details in Ref. [13]. The main characteristics for amorphous In-Se alloys is that the position of the first peak is located between 0.260 and 0.274 nm, which is close to the interatomic distances present in different crystalline phases [13]. Our analysis of the reduced radial distribution functions has concluded that for the same In-Se composition there is a shift of the first nearest-neighbor peak to larger distances with

increasing system density due to higher coordination. In addition, a similar trend for the same system density but increasing indium content was observed.

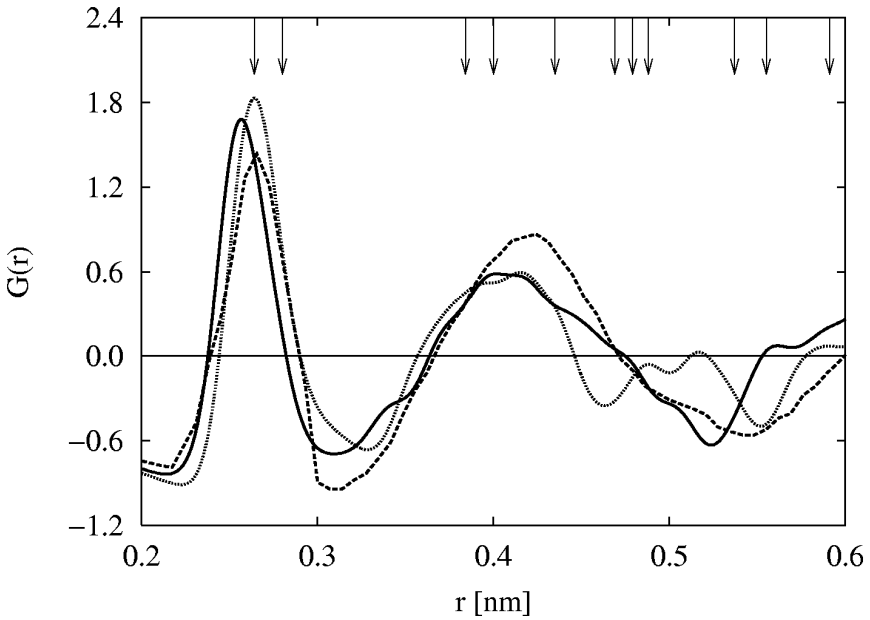

Figure 1. Reduced radial distribution functions of amorphous In_2Se_3 with a density of 5.0 g/cm^3 and amorphous InSe with a density of 5.4 g/cm^3. Solid and dashed lines correspond to data for amorphous In_2Se_3 from our computer simulations and experimental data of Ref. [17], respectively. Dotted line predicts reduced radial distribution function of amorphous InSe. Arrows represent interatomic distances in crystalline β-InSe.

3.2. Coordination numbers

To determine the coordination numbers in amorphous In-Se alloys we used cutoff distances for nearest-neighbors as 0.324, 0.297, and 0.270 nm for In-In, In-Se, and Se-Se bonds, respectively. These numbers correspond to a 12.5% increase of the crystalline covalent diameter and coincide in a satisfactory way with the second minimum in the radial distribution function. We found that in amorphous In-Se alloys on average the coordination number of indium is mainly four and selenium is mostly two- or three-fold coordinated, as seen in Table I. This is in agreement with their crystalline structures [13].

Table I. Average coordination numbers for indium (Z_{In}) and selenium (Z_{Se}) and number of bonds (N_{In-In}, N_{In-Se}, and N_{Se-Se}) for different compositions and densities.

Amorphous	ρ (g/cm^3)	Z_{In}	Z_{Se}	N_{In-In}	N_{In-Se}	N_{Se-Se}
In_2Se_3	5.0	3.3	2.4	3	80	7
	5.4	4.1	2.7	7	93	6
	5.8	4.0	2.7	2	99	3
	6.2	4.1	2.8	4	98	6
InSe	5.0	3.4	2.6	12	84	0
	5.4	3.5	2.7	13	87	0
	5.8	3.8	2.9	15	90	2
	6.2	3.9	3.1	14	98	0
In_4Se_3	5.0	2.5	2.6	10	71	0
	5.4	3.5	2.6	27	71	0
	5.8	3.3	2.8	22	76	0
	6.2	4.0	3.0	32	80	0

We found similar local bonding environments in the amorphous phase as those present in In-Se crystalline alloys, such as In_2Se_3, InSe, and In_4Se_3 [13]. The majority of bonds are heteropolar, but homopolar In-In and Se-Se bonds are also present in the amorphous phase. The general trend is that the number of heteropolar In-In bonds increases with increasing indium content, as illustrated in Table I. This change is however not a linear function of indium content as the amorphous In_4Se_3 alloy (with 57% of indium atoms) has considerably more In-In bonds than the amorphous In_2Se_3 alloy (with 40% indium). Our analysis of the partial coordination numbers has revealed that every indium has on average approximately 0.5, 1.0, and 1.5 nearest-neighbor indium atoms for amorphous In_2Se_3, InSe, and In_4Se_3, respectively [13]. A larger probability for the formation of indium clusters within the amorphous structure might be crucial in explaining the discrepancies between the transport properties of amorphous In-Se alloys with different indium contents [24, 25].

Indium and selenium coordination numbers show large fluctuations in the amorphous sample, as summarized in Table II. This leads to very complicated atomic configurations. Classical random network materials, such as silicon, are known to preserve the coordination number both in the crystalline and amorphous phase with very little or no fluctuations in atomic coordination [26]. We therefore conclude from Table II that amorphous In-Se alloys cannot be considered as classical random network materials.

Table II. Percentage of indium and selenium atoms with different coordination numbers for different compositions and densities. Indium atoms with coordination number of one and two are not shown.

Amorphous	ρ (g/cm^3)	$Z_{In} = 3$	$Z_{In} = 4$	$Z_{In} = 5$	$Z_{Se} = 2$	$Z_{Se} = 3$	$Z_{Se} = 4$
In_2Se_3	5.0	19.2	65.4	0.0	59.0	41.0	0.0
	5.4	3.8	73.1	15.4	33.3	56.4	7.7
	5.8	15.4	73.1	11.5	38.5	53.8	7.7
	6.2	19.2	57.7	19.2	25.6	59.0	12.8
InSe	5.0	15.6	62.5	3.1	43.8	50.0	6.2
	5.4	6.2	62.5	12.5	37.5	53.1	9.4
	5.8	21.9	62.5	9.4	28.1	50.0	21.9
	6.2	3.1	43.8	37.5	12.5	71.9	12.5
In_4Se_3	5.0	16.7	25.0	5.6	37.0	51.9	7.4
	5.4	30.6	41.7	13.9	44.4	48.1	7.4
	5.8	25.0	41.7	11.1	29.6	63.0	3.7
	6.2	33.3	38.9	13.9	22.2	37.0	33.3

3.3. Bond angle distribution function

The bond angle distribution function and ring statistics can also be derived from the detailed knowledge of the amorphous structure. The bond angle distribution function of amorphous InSe with a density of 5.4 g/cm^3 is illustrated in Fig. 2. The position of the main peak is around 100º with a shoulder peak in the vicinity of 120º. This is in agreement with crystalline β-InSe, which has bond angles equal to 98.4º and 119º. The bond angle distribution function possesses a wide distribution with very pronounced tails. The majority of bond angles are between 80º and 130º, but large bond angles can be also found in the amorphous sample. The bond angle distribution functions of other amorphous In-Se alloys with different densities and composition show very similar characteristics to the distribution function shown in Fig. 2 [13]. It can also be concluded from the analysis of the bond angle distribution functions of amorphous In-Se alloys that there is only a very minor contribution to the bond angle distribution function from fragments consisting of two or three nearest-neighbor selenium atoms. In addition, the occurrence of In-In-In fragments in amorphous In_2Se_3 alloys is negligible.

The ring statistics for every amorphous structure can be determined by calculating the shortest closed paths through nearest-neighbor atoms with each bond passed only once [27]. Crystalline In_2Se_3 and InSe contain six-member rings, but in In_4Se_3 five-member rings are also present. Our analysis of the amorphous structures has revealed that the majority of rings belong to these groups, but further four-, seven-, and eight-member rings also exist in the amorphous phase. However, it is likely that a larger number of atoms in the simulation cell will be needed to gain a better insight into the ring statistics of amorphous In-Se alloys.

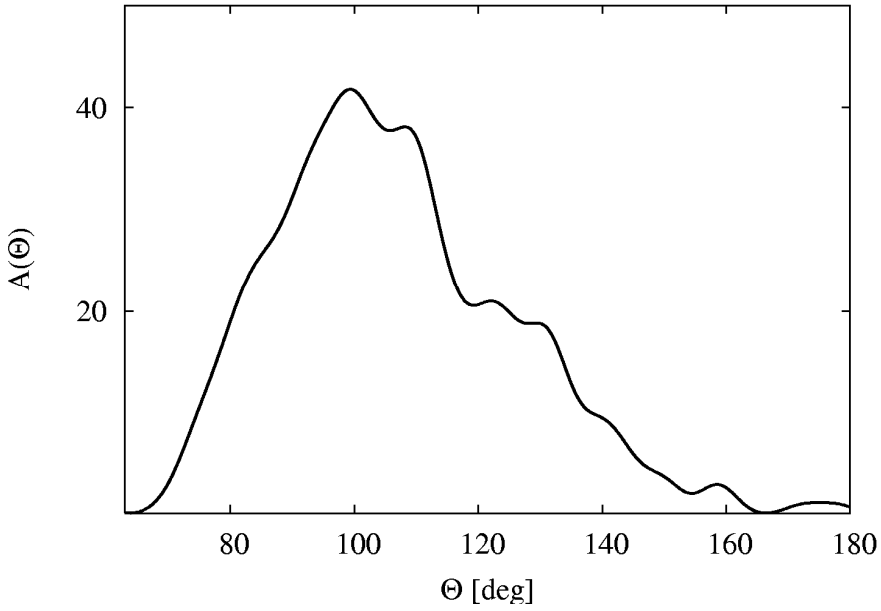

Figure 2. Bond angle distribution function of amorphous InSe with a density of 5.4 g/cm^3.

3.4. Electronic structure

Crystalline and amorphous In-Se compounds are semiconductors with a gap larger than 1 eV. The density of states for β-InSe and for the amorphous InSe with a density of 5.4 g/cm^3 is shown in Fig. 3. The shape of the density of states of the amorphous compound shows similarities to the crystalline density of states, but it has a pseudogap with a finite density of states at the Fermi energy in contrast to experiments. This is probably due to the fact that some liquid defects remained "frozen" during our rapid quench simulations leading to localized states inside the real gap.

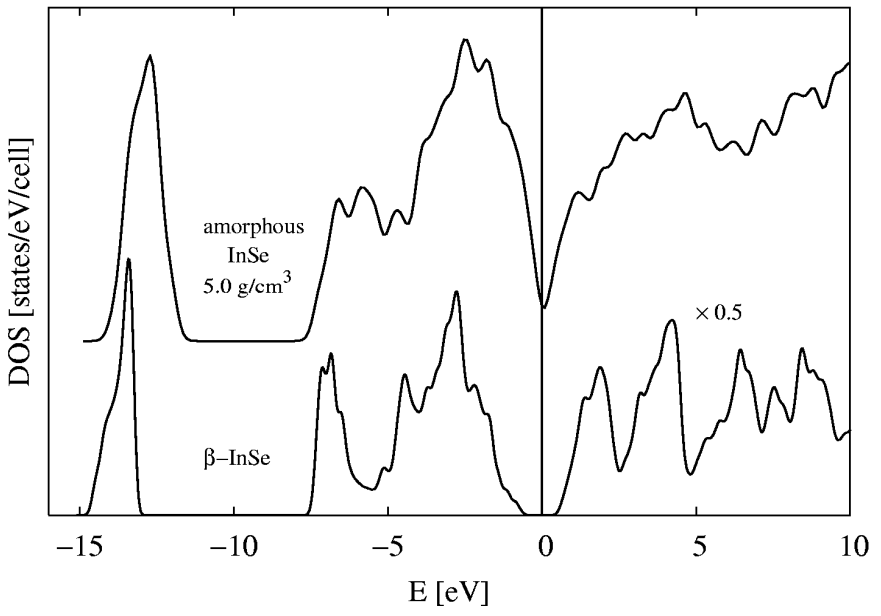

Figure 3. Electronic density of states of β-InSe and amorphous InSe with density of 5.4 g/cm^3. Perpendicular line at zero indicates Fermi energy.

4. Multi-scale modeling

Multi-scale modeling is a very helpful tool to understand and predict device performance of technological applications such as phase-change materials. Multi-scale modeling can provide important information on device optimization from the fundamental point of view and it has the potential to guide and help experimental developments by saving timeless efforts and money investments. The strength of multi-scale modeling is developing models at different length and time scales. In principle, the research spans the entire spectrum from quantum mechanical atomistic simulations through the microscopic scale to macroscopic continuum modeling. But more importantly, it provides understanding about a common problem from the perspective of different disciplines (such as physics, chemistry, materials, and engineering) by finding bridges between modeling hierarchies at different length and time scales (see, for example, Ref. [28]).

Multi-scale modeling of phase-change materials can answer fundamental questions such as the size of the smallest possible amorphous region in a crystalline data storage medium with a lifetime larger than ten years. Recently, we have developed a rate equation model to predict the lifetime of amorphous spots in crystalline matrices for network materials, such as silicon [29]. For the first time this model links re-crystallization processes of the amorphous spot to the underlying structure. Generalization of this model to non-network materials, such as In-Se, could provide information about amorphization and re-crystallization processes of amorphous spots in In-Se alloys. The structural properties of amorphous In-Se alloys, as described in Sec. 3 in this paper, will serve as input parameters for such models. Namely, information on nearest-neighbor bonds, coordination numbers, bond angle distributions and ring statistics can be used in a rate equation model, as there is a strong similarity between the local bonding environment of the amorphous phase and the underlying crystalline structure at the same In-Se composition. In addition, a similar research roadmap of multi-scale modeling of other phase-change materials, such as those based on Ge-Sb-Te alloys, can provide vital information for future data storage applications.

5. Summary

We have performed atomistic simulations of amorphous In-Se alloys in order to study the short-range order of these materials. The local bonding environment of different crystalline In-Se crystal alloys, such as In_2Se_3, InSe, and In_4Se_3 were found to be present in the amorphous phase. We have found a reasonable agreement between the radial distribution function of our amorphous In_2Se_3 sample with a density of 5.0 g/cm^3 and experiment. Our analysis of the atomistic structure of amorphous In-Se alloys has shown that while the coordination number of indium is mainly four, selenium is mostly two- or three-fold coordinated. Large fluctuations in coordination numbers lead to very complicated atomic configurations and therefore amorphous In-Se alloys cannot be considered as classical random network materials. The majority of bonds are heteropolar In-Se bonds, but homopolar In-In and Se-Se bonds are also present in amorphous In-Se alloys. Based on the atomistic information presented in this paper, it is possible to construct models at the continuum level in order to predict the lifetime of In-Se amorphous spots in crystalline materials. Such modeling has already been developed for network materials, such as silicon, and it is possible to generalize these algorithms for non-network materials, such as InSe. Similar multi-scale modeling approaches would be extremely helpful for advanced phase-change materials, such as materials based on Ge-Sb-Te alloys.

Acknowledgements

This research was funded by Hewlett-Packard Laboratories (Palo Alto, California, USA). We acknowledge interesting and valuable discussions with Jim Brug, C.C. Yang, Gary Gibson, Chris Nauka, Alison Chaiken, and Jacek Jasinski. K.K. and D.N.M. would also like to thank Steve Kenny and Andrew Horsfield for helpful discussions regarding PLATO. The calculations were performed using the computer facilities of the Materials Modelling Laboratory and of the Oxford Supercomputing Centre (University of Oxford). K.K. is also grateful for the financial support received from the Data Storage Network of United Kingdom (DSNetUK).

REFERENCES

1. T. Nishida, M. Terao, Y. Miyauchi, S. Horigome, T. Kaku, and N. Ohta, Appl. Phys. Lett. **50**, 667 (1987).
2. G.A. Gibson, A. Chaiken, K. Nauka, C.C. Yang, R. Davidson, A. Holden, R. Bicknell, B.S Yeh, J. Chen, H. Liao, S. Subramanian, D. Schut, J. Jasinski and Z. Liliental-Weber, Appl. Phys. Lett. **86**, 051902 (2005).
3. A. Chaiken, G.A. Gibson, J. Chen, B.S. Yeh, J. Jasinski, Z. Liliental-Weber, K. Nauka, C.C. Yang, D.D. Lindig, and S. Subramanian (in preparation).

4. A. Chaiken, G.A. Gibson, K. Nauka, C.C. Yang, B.-S. Yeh, R. Bicknell-Tassius, J. Chen, J. Jasinski, Z. Liliental-Weber, and D.D. Lindig, presented at the 2003 MRS Fall Meeting (paper HH1.9), Boston, MA, 2003 (unpublished).
5. G.A. Gibson, A. Chaiken, K. Nauka, C.C. Yang, R. Davidson, A. Holden, D.D. Lindig, R. Bicknell-Tassius, J. Chen, H. Liao, D. Neiman, D. Shut, S. Subramanian, B.-S. Yeh, J. Jasinski, Z. Liliental-Weber, presented at the 2003 MRS Fall Meeting (paper HH2.6), Boston, MA, 2003 (unpublished).
6. G. Gibson, T.I. Kamins, M.S. Keshner, S.L. Neberhuis, C.M. Perlov, and Chung C. Yang, US Patent #5,557,596.
7. J. P. Guesdon, B. Kobbi, C. Julien, and M. Balkanski, phys. stat. sol. (a) **102**, 327 (1987).
8. J. F. Sanchez-Royo, A. Segura, O. Lang, E. Schaar, C. Pettenkofer, R. Roa, and A.Chevy, J. of Appl. Phys. **90**, 2818 (2001).
9. C. Julien, I. Samaras, M. Tsakiri, P. Dzwonkowski, and M. Balkanski, Mat. Sci. and Eng. B **3**, 25 (1989).
10. V.K. Lukyanyuk, M.V. Tovarnitskii, and Z. D. Kovalyuk, phys. stat. sol. (a) **104**, K41 (1987).
11. D. Fargues, G. Tyuliev, G. Brojerdi, M. Eddrief, and M. Balkanski, Surf. Sci. **370**, 201 (1997).
12. T. Ohta and S.R. Ovshinsky, "Phase-Change Optical Data Storage Media," p. 310-326, in *Photo-Induced Metastability in Amorphous Semiconductors*, Ed. by A..V. Kolobov (Wiley-VCH, New York, 2003).
13. K. Kohary, V.M. Burlakov, D.G. Pettifor, and D. Nguyen-Manh, Phys. Rev. B **71**, 184203 (2005).
14. K. Imai, K. Suzuki, T. Haga, Y. Hasegawa, and Y. Abe, J. Cryst. Growth **54**, 501 (1981).
15. A. Jablonska, A. Burian, A.M. Burian, J. Szade, O. Proux, J.L. Hazemann, A. Mosset, and D. Raoux, J. of Non-Cryst. Sol. **299-302**, 238 (2002).
16. A. Jablonska, A. Burian, A.M. Burian, P. Lecante, and A. Mosset, J. of Alloys and Compounds **328**, 214 (2001).
17. A. Burian, A.M. Burian, J. Weszka, M. Zelechower, and P. Lecante, J. of Mat. Sci. **35**, 3121 (2000).
18. D. Drabold and J. Li, Curr. Op. in Sol. State and Mat. Sci. **5**, 509 (2001).
19. S. Popovic, A. Tonejc, B. Grzeta-Plenkovic, B. Celustka, and R. Trojko, J. Appl. Cryst. **12**, 416 (1979).
20. S.D. Kenny, A.P. Horsefield, and H. Fujitani, Phys. Rev. B **62**, 4899 (2000).
21. A.P. Horsfield, Phys. Rev. B **56**, 6594 (1997).
22. S. Goedecker, M. Teter, and J. Hutter, Phys. Rev. B **54**, 1703 (1996).
23. C. Hartwigsen, S. Goedecker, and J. Hutter, Phys. Rev. B **58**, 3641 (1998).
24. S. Marsillac, J.C. Bernede, and A. Conan, J. Mater. Sci. **31**, 581 (1996).
25. A. Chaiken, K. Nauka, G.A. Gibson, H. Lee, and C.C. Yang, J. Appl. Phys. **94**, 2390 (2003).
26. P.K. Gupta, J. Non-Cryst. Solids **195**, 158 (1996).
27. D.S. Franzblau, Phys. Rev. B **44**, 4925 (1991).
28. D.G. Pettifor, Acta Materialia **51**, 5649 (2003).
29. K. Kohary, V.M. Burlakov, and D.G. Pettifor, Phys. Rev. B **71**, 235509 (2005).